Clay Minerals (2019), **54**, 145–151
doi:10.1180/clm.2019.23

CAMBRIDGE UNIVERSITY PRESS

Article

Impregnation of silver in zeolite–chitosan composite: thermal stability and sterility study

Kathrina Lois M. Taaca*, Eleanor M. Olegario and Magdaleno R. Vasquez Jr
Department of Mining, Metallurgical, and Materials Engineering, College of Engineering, University of the Philippines-Diliman, Quezon City, 1101 Philippines

Abstract

The solvent-casting method was used to synthesize a silver–zeolite–chitosan (AgZ-Ch) composite from Philippine natural zeolites. X-ray diffraction, ultraviolet–visible (UV-Vis) spectroscopy, optical emission spectroscopy (OES), thermogravimetric analysis (TGA) and differential thermogravimetry (DTG) were used to investigate the different properties of the composite before and after plasma treatment. The major phase of the zeolite is Na-clinoptilolite with trace amounts of mordenite, feldspar and quartz. UV-Vis and OES analyses confirmed the presence of Ag and zeolite on the chitosan matrix. The decrease in the transmittance signal at 290 nm and the emission spectra of the discharge showed the presence of Ag I, Al I and Si I signals at 705–852 nm. The TGA and DTG curves revealed the thermal stability of the natural zeolites after ion exchange and after incorporation in the chitosan matrix, where the onset of degradation was observed to occur above ~37°C, the human body temperature. Bacterial count showed minimal growth of colonies on all samples, both pristine and plasma-treated, suggesting that the surface of the composites does not influence bacterial habitation. The fabricated composites meet the minimum requirements for biomedical application such as thermal stability with respect to the average human body temperature and absence of bacteria.

Keywords: surface interactions, silver, zeolites, chitosan, plasma, degradation, transmittance

(Received 4 August 2018; revised 3 March 2019; Accepted Manuscript online: 24 May 2019; Guest Associate Editor: A. Dakovic)

Aluminosilicate minerals have previously been used in traditional medicine and pharmaceutical industries (Boniferri *et al.*, 2007; Ghadiri *et al.*, 2015). Specifically, clay minerals are among the oldest earth materials employed for traditional healing purposes, as indigenous peoples around the world use them externally, primarily in baths to cure skin diseases and simple gastrointestinal ailments such as diarrhoea (Ghadiri *et al.*, 2015). Clay minerals are often used in modern-day applications due to their many advantages, including their high adsorption and cation-exchange capacity (CEC), colloidal and swelling capacity, optimal rheological behaviour and high water dispersibility. These physicochemical characteristics are identified as being essential in a wide range of biological applications, such as veterinary medicine, pharmaceutics, cosmetics, biomaterials and biosensors (Ghadiri *et al.*, 2015). Moreover, clay minerals may generally serve as carriers, binders or diluent agents for these industrial applications (Cerri *et al.*, 2004).

Besides clays, zeolites are also considered to be amongst the most abundant natural resources in the world. Zeolites have similar properties to clays, although they have different structural features. They are tectosilicates, microporous molecular sieves in which the silicon (Si)–aluminium (Al) tetrahedra are linked by bridges of oxygen (O) (Ferreira *et al.*, 2012). The zeolite structure has interconnected voids and channels that host extra-framework cations in cation-exchange sites. These cations are replaced when the zeolites are immersed in a solution containing other exchangeable cations (Ferreira et al., 2012). This cation-exchange mechanism of zeolites is similar to that observed in clay minerals (Cerri *et al.*, 2004; Bonferoni *et al.*, 2007). Adsorption and reversible dehydration are some of the other significant properties shared by zeolites and clays that make them indispensable in industrial and biological applications (Cerri *et al.*, 2016).

Research on zeolites for biological applications has become an area of increasing interest. Studies on the biomedical use of zeolites are relatively new compared to similar studies using clays. In fact, the quality of clays for biological applications has been established by several studies. For instance, the pharmaceutical use of clays has been specified in pharmacopoeia standards (European Pharmacopoeia, 2005; Tomasevic-Canovic, 2005; US Pharmacopeia, 2007; Carretero & Pozo, 2009; Alkrad *et al.*, 2017; Dardir *et al.*, 2018). It is projected that the utilization of zeolites, specifically Philippine natural zeolites, will be maximized in the future due to their well-defined structures, ability to reversibly bind to small molecules, shape and size selectivity, metallo-enzyme behaviour and immune system regulatory properties (Inoue *et al.*, 2002; Demirci *et al.*, 2013; Cerri *et al.*, 2016). Zeolites may act as inorganic reservoirs for hosting ions such as zinc (Zn) (Olegario-Sanchez & Pelicano, 2017; Olegario *et al.*, 2019), copper (Cu) (Montallana *et al.*, 2018) and silver (Ag) (Osonio & Vasquez Jr, 2018) and thereby prevent possible concentration-dependent toxicity as well as control and regulate ionic release for antibacterial applications (Ferreira *et al.*, 2012). The rigid and stable structure of zeolites allows for functions in nanotechnology, heterogeneous

*E-mail: kmtaaca@up.edu.ph
This paper was submitted to the 10th International Conference on the Occurrence, Properties, and Utilization of Natural Zeolites (Krakow, June 2018).
Cite this article: Taaca KLM, Olegario EM, Vasquez Jr MR (2019). Impregnation of silver in zeolite–chitosan composite: thermal stability and sterility study. *Clay Minerals* **54**, 145–151. https://doi.org/10.1180/clm.2019.23

catalysis, ion exchange and sorption (Ferreira *et al.*, 2012). In addition, zeolites are promising carriers for drug-delivery systems because of their excellent adsorption and CEC. They may interact with various molecules and, due to their porous structure, may transfer atoms or molecules to the environment and *vice versa* (Barbosa *et al.*, 2016; Taaca & Vasquez Jr, 2017).

Zeolites dispersed as fillers in a polymer matrix have been studied in biomedical applications (Ciobanu *et al.*, 2007; Namekawa *et al.*, 2014; Ramasubramanian *et al.*, 2015; Barbosa *et al.*, 2016; Taaca *et al.*, 2017; Taaca & Vasquez Jr, 2018). Several zeolite-based composites have been fabricated using extrusion, melt mixing, compounding, freeze drying, precipitation and cross-linking. These composites include hydroxylapatite/zeolite-ZSM5 (ZSM-HA) (Iqbal *et al.*, 2016), titanium/MFI zeolite (M-Ti) (Li *et al.*, 2015) and gelatin/zeolite (Ninan *et al.*, 2013). The bioactivity of ZSM-HA was demonstrated when normal human osteoblasts adhered to and proliferated on the surface of the composites (Iqbal *et al.*, 2016). Ti alloys coated with MFI zeolites have enhanced osteointegration and promoted bone regeneration when implanted in rabbit femoral condylar defects at 4 and 12 weeks (Li *et al.*, 2015). The porosity, swelling and degradation properties of the zeolite–gelatin scaffold showed potential for regenerative medicine and tissue engineering (Ninan *et al.*, 2013).

In our previous work, a composite made from Ag-exchanged zeolite (AgZ) and chitosan (Ch) was fabricated successfully using a solvent-casting approach. Its antibacterial, cytocompatibility and haemocompatibility properties were evaluated for possible biomedical applications (Taaca & Vasquez Jr, 2017, 2018). In addition, there are previous studies focusing on Ch–zeolite composites for biomedical application (Yu *et al.*, 2013; Zhang *et al.*, 2015). However, surface modification *via* plasma treatment to tailor the surface properties of the composite has scarcely been reported, although it has been considered an effective method for enhancing the wettability and surface roughness of polymers, such as Ch, and ceramic materials, such as zeolites (Cagomoc & Vasquez Jr, 2016; Osonio & Vasquez Jr, 2018). The porosity and the surface properties (roughness and wettability) of Ch were greatly enhanced with the presence of AgZ particles coupled with plasma treatment (Taaca & Vasquez Jr, 2017). In addition, the AgZ fillers enhanced not only the antibacterial activity of Ch, but also its blood-clotting ability, without promoting adverse effects (Taaca & Vasquez Jr, 2018).

In this study, composites of AgZ-Ch were synthesized and their thermal responses evaluated. In addition, the presence of microorganisms in the composite surface was investigated. Local natural zeolites were characterized with X-ray diffraction (XRD). The properties of the composites were determined using thermogravimetric analysis (TGA) and UV-Vis spectroscopy. The gas discharge was analysed with optical emission spectroscopy (OES).

Materials

The zeolite samples, supplied by SAILE Industries, Inc., were mined in the town of Mangatarem, province of Pangasinan, Philippines. The samples were pre-treated to produce sodium-exchanged zeolite (NaZ). Medium-molecular-weight (44487-50G) Ch was purchased from Sigma-Aldrich. Analytical-grade acetic acid (CH_3COOH) from Macron, locally sourced 99% silver nitrate ($AgNO_3$) and glycerine and isopropyl alcohol were also procured for the synthesis of the composites. All materials were used as received unless specifically mentioned in the succeeding steps. Deionized water (DI H_2O) was used throughout the experimental runs.

Methods

Ion exchange

The ion-exchange method used in this study follows previous work (Taaca & Vasquez Jr, 2017, 2018). The as-received NaZ minerals were ground with a pestle and mortar, washed with 100 mL of DI H_2O and filtered twice after each washing step. The washed powders were dried at 105°C for 2 h and heated at 120°C for 6 h. The ion-exchange process started by soaking the actively treated NaZ powders in a 0.05 M $AgNO_3$ solution at room temperature (RT) overnight, with a NaZ powder:$AgNO_3$ solution ratio of 1:20 (w/v). The mixture was then stirred vigorously for an additional 12 h to continue the ion-exchange process at RT. The AgZ obtained was washed and filtered. These steps were performed twice after the ion-exchange process. The filtered AgZ was dried at 105°C for 2 h. After the ion-exchange process, the samples were calcined at 400°C for 5 h to reduce the Ag^+ ions impregnated in the zeolite channels to metallic Ag. Metallic Ag is effective as an antibacterial agent due to the regulated release of Ag^+ ions (Xiu *et al.*, 2012; Osonio & Vasquez Jr, 2018).

Synthesis of AgZ-Ch composites

The AgZ-Ch composites were prepared by mixing the Ch and the zeolite suspensions *via* the solvent-casting method for 2 h (Taaca & Vasquez Jr, 2017). The Ch suspension consisted of 2 wt.% Ch and 90% CH_3COOH solution stirred (380 rpm) at 60°C. The AgZ suspension was prepared by dispersing 5% (w/v) AgZ in DI H_2O sonicated for 30 min. Different AgZ-Ch mixtures were prepared by adding varying amounts of zeolites (0–2.0 wt.%) and mixing for another 1 h. Glycerine was also added as a plasticizer to each of the AgZ-Ch mixtures. The mixtures were then cast on a polystyrene Petri dish and air-dried for 2–3 days. The dried AgZ-Ch films were soaked in an isopropyl alcohol solution for 1 h as a post-treatment step. The final dried samples were sealed in a desiccator prior to plasma treatment.

Plasma treatment of the AgZ-Ch composites

The plasma setup is similar to the system used in previous studies of local natural zeolites (Cagomoc & Vasquez Jr, 2016; Taaca & Vasquez Jr, 2017, 2018; Osonio & Vasquez Jr, 2018). The plasma system utilizes a 13.56 MHz radiofrequency (RF) power with a manually tuned matching network. For all runs, 99.99% argon (Ar) gas was used. Prior to treatment, the system was cleaned with plasma to remove possible gas impurities present inside the chamber.

Selected dried films of AgZ-Ch composites (0% AgZ-Ch and 1.0% AgZ-Ch) were exposed to Ar plasma after chamber cleaning in order to determine the effect of plasma discharge on the composites with or without AgZ. The plasma system was first evacuated to base pressures below 10 Pa. The experiments were conducted under an incident RF power of 50 W and pressures of 16 and 30 Pa for 2 min. Low pressure was used to modify the surface properties of the AgZ-Ch composites without significantly affecting the bulk properties.

Characterization

The composition of the zeolite phases of the as-received NaZ sample was determined by XRD with a Shimadzu Maxima XRD-7000 diffractometer with a scan speed of 0.02°/min in the range $2\theta = 2°–70°$. The NaZ powder samples were pressed on

https://doi.org/10.1180/clm.2019.23 Published online by Cambridge University Press

double-sided tape and mounted on a glass slide prior to characterization. The composites were examined using a PANalytical X'Pert diffractometer with a continuous scan mode in the range 2θ = 5°–80°. The thermal stability of AgZ and the AgZ-Ch composites was evaluated by TGA using a TGA Q500 analyser (TA Instruments) under a dynamic N_2 atmosphere (100 mL/min) in the temperature range 30–700°C at a heating rate of 10°C/min. The UV-Vis absorption spectra of the AgZ-Ch composites were collected with a Shimadzu UVmini-1240 spectrometer. The baseline of the UV-Vis analysis was corrected to 200 nm with a scanning range of 0–1200 nm. The ionic species detected in the plasma discharges during the plasma treatment of the composites at various working pressures were analysed by OES using an Horiba iHR320 spectrometer. Analysis of the bulk plasma was performed using *Spectral Analyzer 1.7* software (Navratil *et al.*, 2006). The spectrum of the discharge in each step was observed for any changes throughout the process.

Bacteria counts of the pristine and selected plasma-treated AgZ-Ch composites were performed in the Microbiological Research and Services Laboratory (MRSL) of the Natural Sciences Research Institute (NSRI) in the University of the Philippines-Diliman. The composites were washed with 9 mL of 0.1% peptone water for 2 min. The washings were diluted up to a dilution factor of 10^{-2}. Dilutions were pour-plated in plate count agar in duplicate. Plates were incubated at 35°C for 48 h before counting the colonies under a Quebec colony counter. The weighted mean count (WMC) was expressed as colony-forming units (CFU) per gram of sample and was calculated using the formula in Eq. 1:

$$WMC = \frac{n}{(f_a \times 1) + (f_b \times 0.1) + (f_c \times 0.01) + \ldots} \times df \qquad (1)$$

where n represents the total number of counted colonies in all plates, f_a is the number of plates with the first countable dilution, f_b and f_c are the numbers of plates in the succeeding dilutions and df is the dilution factor, which is equal to the reciprocal of f_a. For all characterizations, 1 cm × 1 cm dried sheets of AgZ-Ch composites and 3 μg of zeolite were used.

Results and discussion

XRD results of as-received NaZ and the AgZ-Ch composites

The XRD trace of the as-received NaZ sample is shown in Fig. 1. The natural zeolite is composed of Na-clinoptilolite (Alberto, 1975), mordenite (Martucci *et al.*, 2003), feldspar (Grundy & Ito, 1974) and quartz (Levien *et al.*, 1980). The presence of other zeolite peaks is possible as no purification of the natural zeolite samples prior to exchange of Na^+ ions was done. Figure 2 shows the XRD traces for the pristine AgZ-Ch composites. Chitosan has a broad characteristic peak at 20–25°2θ, centred at approximately 21°2θ (Taaca & Vasquez Jr, 2018). The characteristic peak of Ch did not change significantly upon the addition of AgZ particles (Fig. 2).

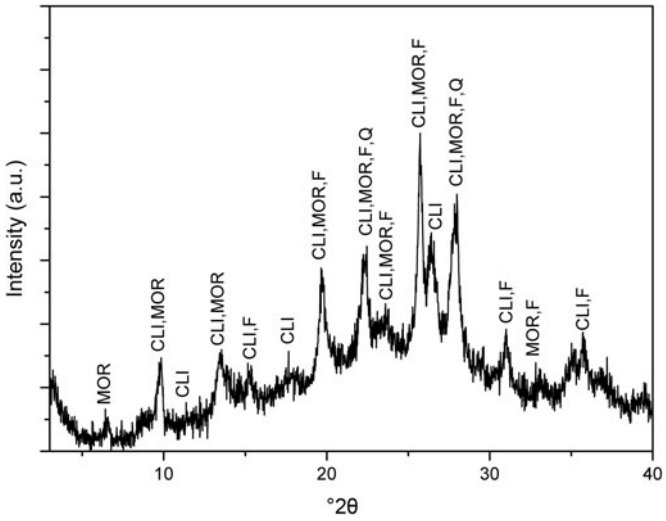

Fig. 1. XRD trace of the as-received NaZ sample. Characteristic peaks correspond to Na-clinoptilolite (CLI), mordenite (MOR), feldspar (F) and quartz (Q).

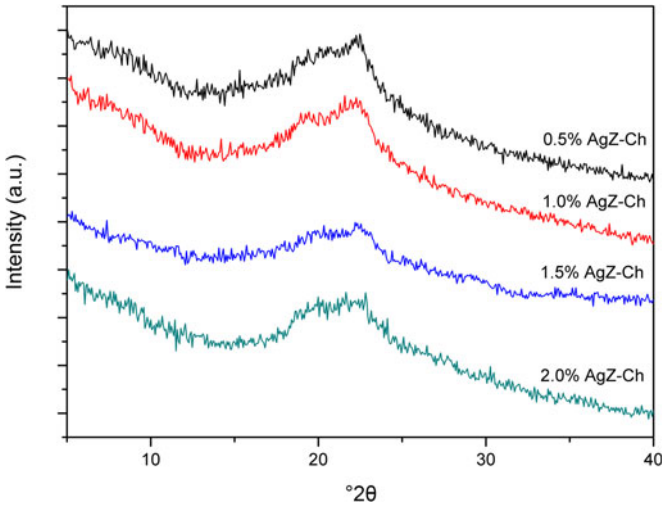

Fig. 2. XRD traces of the pristine AgZ-Ch composites with varying AgZ contents (0.5–2.0%).

UV-Vis analyses of the AgZ-Ch composite samples

UV-Vis spectrometry was used to detect the presence of AgZ in the AgZ-Ch composites. The pure Ch, 0% AgZ-Ch composite has characteristic signals at 240 and 290 nm (Fig. 3). These signals may be attributed to the glucosamine unit of Ch and the chemical interaction of CH_3COOH and Ch at RT, respectively. Decreasing intensities of the transmittance signal at 290 nm are observed after incorporating 0.5–2.0 wt.% of AgZ powders into the Ch matrix. The intensity values changed from 79.32 to 1.06–68.70. In addition, the decreasing trend of the transmittance with increasing AgZ content indicates that AgZ particles in the matrix increase UV absorption, for which the 2.0 wt.% AgZ-Ch composite has the lowest transmittance value of 1.06, in accordance with previous similar studies (Concepcion-Rosabal *et al.*, 2005). The spectra also confirmed that Ag was successfully incorporated in the zeolite. The AgZ clusters in the composites may also act as scattering points that reduce the intensity of transmitted light. This reduction provides insights into the dispersibility of the AgZ particles in the polymer matrix.

Assessment of the thermal properties of the AgZ and AgZ-Ch composite samples

The TG and DTG curves of the AgZ samples are shown in Fig. 4. The AgZ sample displayed continuous weight loss of ~10 wt.%

https://doi.org/10.1180/clm.2019.23 Published online by Cambridge University Press

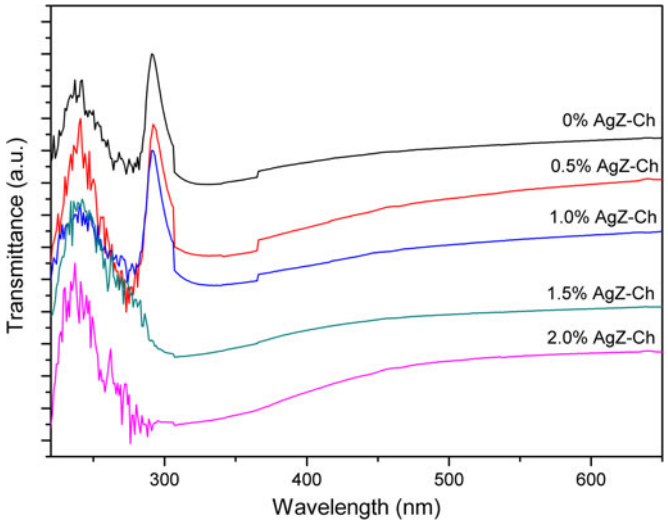

Fig. 3. UV-Vis transmittance spectra of AgZ-Ch composites at different AgZ contents.

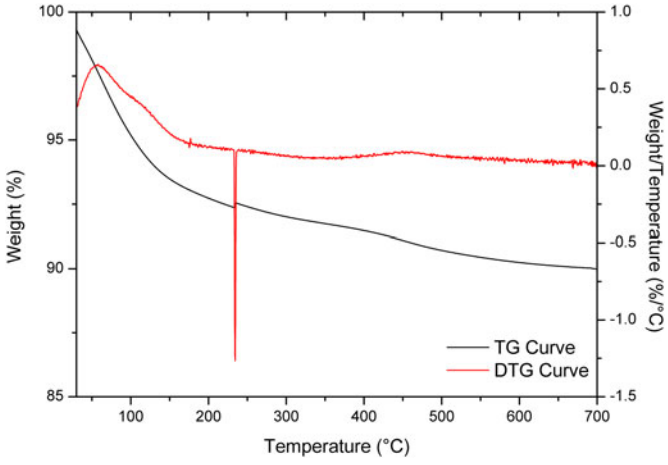

Fig. 4. TG and DTG curves for AgZ samples.

over the temperature range of 25–700°C. The degradation of AgZ was monitored from the endothermic DTG events at 45.5°C, 234.1°C and 442.7°C. The smooth and continuous TG curve of the AgZ sample is similar to what has been found in previous works (Akdeniz & Ulku, 2008; Mansouri *et al.*, 2013), suggesting that the structure of zeolite did not change upon dehydration. The degradation of the as-received NaZ sample, on the other hand, was observed over the temperature range of 104–662°C (Olegario-Sanchez, 2016). This indicated that the incorporation of Ag into the zeolite caused the onset of degradation to shift to lower temperatures.

Figure 5 shows the TG and DTG curves of the AgZ-Ch composites. Pure Ch has two degradation steps. The first step is observed at 60°C due to the water loss in the Ch structure. The second major weight loss of Ch is located at 300°C (Uygun *et al.*, 2011). The onsets of degradation of the composites are clearly shown in the DTG curves. For the AgZ-Ch composites, three degradation steps were observed. The peak temperatures and amount of weight lost for each AgZ-Ch composite are summarized in Table 1. The addition of AgZ to the Ch structure shifted its onsets of degradation to lower values. The water loss is greater in the 0.5% AgZ-Ch composite. Overall, the 1.0% AgZ-Ch composite has the least amount of residue remained after heating.

Optical emission spectroscopy analyses of the discharge

The OES analysis was used to probe the gas discharges in this study. Figures 6 and 7 display the OES images of 0% AgZ-Ch and 1.0% AgZ-Ch composites exposed at 16 and 30 Pa Ar plasma discharges, respectively. The intensity of the plasma discharges of the composites varied from 0 to 6500 cps measured in the wavelength range of 0–1000 nm. In both OES spectra of the 0% AgZ-Ch composite (16 and 30 Pa), the dominant species were C, CO, N, N_2, NH, O_2 and Ar (Navratil *et al.*, 2006), attributed to the possible dissociation of C, H, O and N species from the Ch after plasma treatment. In addition, the spectra of 1.0% AgZ-Ch composites treated at 16 and 30 Pa showed that Al peaks dominated the carbon I, and O_2 radical I peaks at wavelengths 736 and 762 nm, respectively (Navratil *et al.*, 2006). The Ag and Si peaks were also observed at 705 and 852 nm, respectively. In summary, additional peaks were observed in both 1.0% AgZ-Ch spectra due to Al, Ag and Si species (Navratil *et al.*, 2006). This confirmed the presence of AgZ in the 1.0% AgZ-Ch composites and, specifically, the presence of Ag in the zeolite minerals.

Bacteria count in the pristine and plasma-treated pure Ch film

The results of the bacterial counts are summarized in Table 2. The pristine 0% AgZ-Ch composite does not have any bacterial inhabitants on its surface (<10 CFU/cm^2 was recorded). Hence, the apparatus and glassware used to prepare the composite were sterilized to avoid bacterial colonization on the surface. In addition, the soaking of the 0% AgZ-Ch composites in an isopropyl alcohol solution might have caused disinfection on the surface of the composite. Plasma-treated 0% AgZ-Ch composites were also investigated. Plasma treatment is also considered to be a sterilization method as it relies on specific active agents, such as UV photons and radicals (Moisan *et al.*, 2002). No more than 10 CFU/cm^2 was observed in the plasma-treated AgZ-Ch composites. This revealed that plasma modification does not initiate bacterial colonization on the AgZ-Ch composites. Further investigation could focus on evaluating the effectiveness of plasma treatment for sterilization against test microorganisms.

Discussion

The natural zeolite from the Philippines used in this study was composed mainly of clinoptilolite and mordenite, followed by feldspar and quartz. The zeolite was in the Na form due to the high exchangeability of Na^+ ions when immersed in aqueous solution (Ferreira *et al.*, 2012; Demirci *et al.*, 2013). The characteristic peak of Ch did not seem to change with the presence of AgZ particles. The absence of Ag and AgZ peaks in the XRD patterns of the composite might be due to their very small particle sizes that cannot be detected by XRD. The effect of particle-size distributions on natural zeolites has been observed in previous studies that determined the minimum radius limit of the XRD, small-angle X-ray scattering, and UV-Vis characterization techniques (Concepcion-Rosabal *et al.*, 2005).

In the present study, UV-Vis was used in combination with XRD to further characterize Ag and AgZ particles in the composites. The Ag peak, expected at 37.16°2θ, might not be clearly

https://doi.org/10.1180/clm.2019.23 Published online by Cambridge University Press

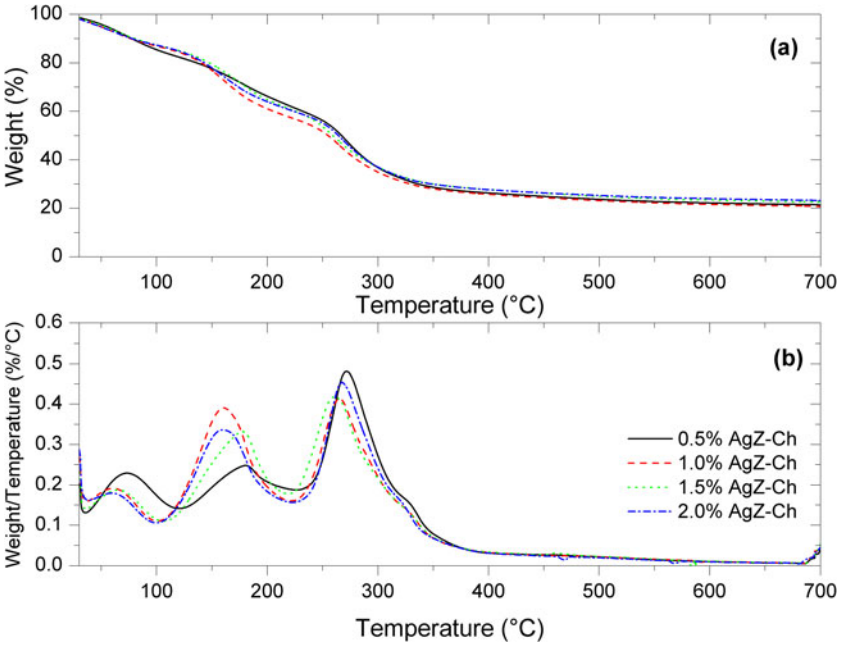

Fig. 5. (a) TG and (b) DTG curves of 0.5%, 1.0%, 1.5% and 2.0% AgZ-Ch composites.

Table 1. Summary of the weight loss of the AgZ-Ch composites.

	First step		Second step		Third step	
AgZ content (%)	Peak temperature (°C)	Weight loss (%)	Peak temperature (°C)	Weight loss (%)	Peak temperature (°C)	Weight loss (%)
0.5	60.90	17.49	167.61	21.73	267.73	36.86
1.0	48.55	13.15	153.71	29.58	259.81	33.70
1.5	46.10	13.49	171.71	25.46	255.87	34.89
2.0	44.37	12.66	153.33	27.12	266.41	34.68

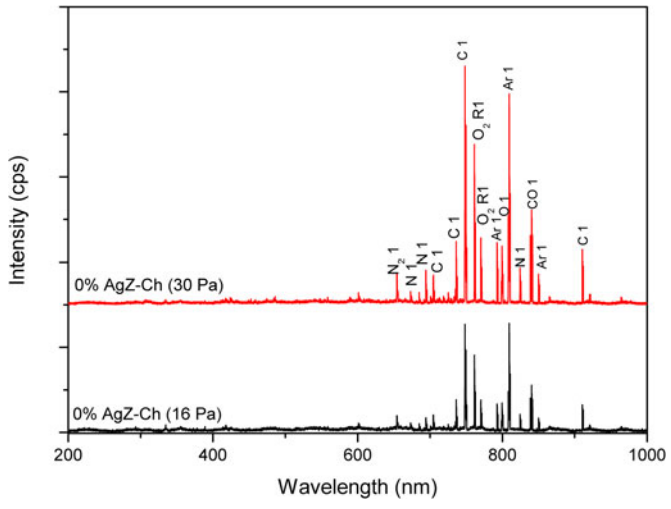

Fig. 6. OES spectra of 0% AgZ-Ch composites exposed to 16 and 30 Pa Ar plasma discharges.

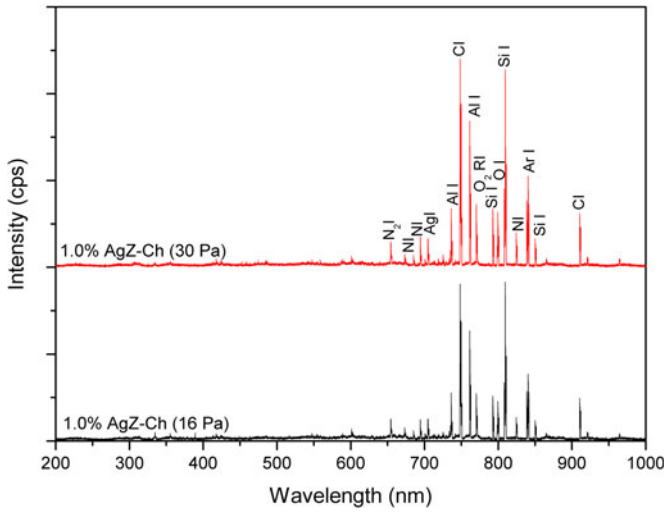

Fig. 7. OES spectra of 1.0% AgZ-Ch composites exposed to 16 and 30 Pa Ar plasma discharges.

detected in the XRD trace of the AgZ sample as the peak also corresponds to a zeolitic peak (Taaca & Vasquez Jr, 2017). Yet there was antibacterial activity observed in the AgZ sample against *Escherichia coli* and *Staphylococcus aureus* (Taaca & Vasquez Jr, 2018). Natural clinoptilolites with Ag (Ag-NC), reduced at 400°C, may have characteristic XRD peaks of metallic Ag between 37°2θ and 45°2θ (Concepcion-Rosabal *et al.*, 2005). These peaks might be attributed to large Ag particles located outside of the clinoptilolite and mordenite channels after reduction at 400°C. Furthermore, several types of Ag clusters might form in zeolites

https://doi.org/10.1180/clm.2019.23 Published online by Cambridge University Press

Table 2. Bacterial counts of 0% AgZ-Ch film washings in concentrations of 10^{-1} and 10^{-2} dilution factors.

0% AgZ-Ch sample	CFU/cm^2
Untreated	<10
16 Pa	<10
30 Pa	<10

with different molar SiO_2/Al_2O_3 ratios (Bogdanchikova *et al.*, 1999). Different Ag clusters are assigned to different optical spectral wavelength peaks. The signal at 290 nm is assigned to the clusters of positively charged Ag_8^{m+} or Ag_7^{m+} (Bogdanchikova *et al.*, 1999). In this study, the transmittance peak at 290 nm decreased with increasing AgZ content. The disappearance of the transmittance peak may imply that absorbance increases with increasing AgZ content. This indicates that the formation of Ag_8^0, due to the reduction of the Ag_8^{m+} and Ag_7^{m+}, becomes better defined and stabilized at higher AgZ contents. Furthermore, calcination as a reduction process to Ag particles produced several Ag clusters inside the zeolite pores and can only be observed by UV-Vis spectroscopy.

In addition to UV-Vis, OES was also utilized where an Ag I peak was observed at 705 nm. The detection of an Ag peak after plasma treatment would signify that the type of Ag present in the AgZ-Ch composites is from the cluster of positively charged Ag_8^{m+} or Ag_7^{m+}. The plasma treatment was performed at low pressures, yet OES analyses displayed an Ag peak at intensities of <1500 cps, implying that Ag ions were not completely reduced by calcination to Ag_8^0, but remained partly in the positively charged state. It is recommended that the calcination step be improved or other reduction process utilized, such as plasma treatment (Nolan *et al.*, 2018; Osonio & Vasquez Jr, 2018), to reduce Ag^+ ions to Ag^0 particles. The Ag^0 state is more suitable for antibacterial applications due to its morphological and physicochemical characteristics, which influence its antibacterial activity in addition to its ability to control the release of ions (Dizaj *et al.*, 2014).

The degradation of samples was caused by dehydration of the zeolites, similar to findings in other studies (Mansouri *et al.*, 2013). The observed onsets of modification might be attributed to the removal of hygroscopic water and loosely bonded water from clinoptilolite (Mansouri *et al.*, 2013). The onset of modification of AgZ indicates that it is suitable for biomedical applications. The AgZ synthesized by ion exchange did not reveal any changes in the composition and structure of the zeolites. The effect of Ag was observed in the TGA results, showing that the thermal degradation of AgZ occurs at lower temperatures than for NaZ. Despite this decrease, compared to the pure Ch sample, the composites still meet the thermal requirements for a biomaterial or an implant. As the onset of degradation occurs at 44.37–60.90°C, the composites have good thermal stability and may support physiological functions inside the human body where the normal temperature is ~37°C.

Sterilization physically or chemically eliminates all types of microorganisms (Moisan *et al.*, 2002). Plasma sterilization relies on photons and radicals to actively react with various microorganisms. Plasma treatment was performed previously on AgZ-Ch composites in order to modify their surface properties, such as wettability and surface roughness (Taaca & Vasquez Jr, 2017). In the present study, the possible effect of plasma treatment as a sterilization technique was examined. The test revealed that <10 CFU/cm^2 was observed at all samples, suggesting that the AgZ-Ch composite may readily be used as an implant without concern regarding its sterility, as bacterial colonies are at a minimum. Similar properties were observed for plasma-treated AgZ-Ch composites because all of the samples were soaked in an isopropyl alcohol solution prior to plasma treatment. It is recommended that the effect of plasma treatment as a sterilization technique be further investigated for this particular material.

Summary and conclusions

AgZ-Ch composites were fabricated using a solvent-casting approach. The zeolite sample consisted of Na-clinoptilolite with traces of mordenite, quartz and feldspar. UV-Vis analysis demonstrated a decrease in the transmittance peaks, especially at 290 nm, implying that AgZ particles are present in the AgZ-Ch composites. The decrease in transmittance denotes that there is an increase in the absorbance at 290 nm, suggesting that the reduction of Ag ions becomes more defined and stabilized with higher concentrations of AgZ. The OES spectra displayed an Ag I peak at 705 nm with lower intensity, suggesting that some of the Ag present in the composites was not reduced and therefore was dissociated from the composite when exposed to the Ar plasma discharge. The presence of AgZ in the composite shifted the onset of degradation to occur at lower temperatures, but still >37°C, the typical temperature of a human body. The AgZ-Ch composites – both pristine and plasma-treated – are safe for use as biomaterials applied either topically or as implants as the surfaces of these composites did not serve as habitats for microorganisms. The synthesized AgZ-Ch composites – both pristine and plasma-treated – meet the minimum requirements for a biomaterial.

Author ORCIDs. K.L.M. Taaca, 0000-0001-7648-0870

Acknowledgements. K.L.M. Taaca acknowledges the support of the Engineering Research for Development and Technology scholarship grant and the National Institute of Physics (NIP) in the University of the Philippines-Diliman for the UV-Vis characterization, as well as Doshisha University in Japan for the XRD characterization of the composites. M.R. Vasquez Jr is grateful to the University of the Philippines Office of the Vice President for Academic Affairs Balik-PhD Grant (OVPAA-BPhD-2014-01) and the Jardiolin Family Professorial Chair. The authors also thank SAILE Industries, Inc., for the zeolite samples.

References

Akdeniz Y. & Ulku S. (2008) Thermal stability of Ag-exchanged clinoptilolite rich mineral. *Journal of Thermal Analysis and Calorimetry*, **94**, 703–710.

Alberto A. (1975) The crystal structure of two clinoptilolites locality: Alpe di Siusi, Italy. *Tschermaks Mineralogische und Petrographische Mitteilungen*, **22**, 25–37.

Alkrad J., Shmeis R., Alshwabkeh I., Abazid H. & Mohammad H.A. (2017) Investigation of the potential application of sodium bentonite as an excipient in formulation of sustained release tablets. *Asian Journal of Pharmaceutical Sciences*, **12**, 259–265.

Barbosa G., Debone H., Severino P. & da Silva C. (2016) Design and characterization of chitosan/zeolite composite films effect of zeolite type and zeolite dose on the film properties. *Materials Science and Engineering C*, **60**, 246–254.

Bogdanchikova N., Petranovskii V., Machorro R., Sugi Y., Soto V.M. & Fuentes S.M. (1999) Stability of silver clusters in mordenites with different SiO_2/Al_2O_3 molar ratio. *Applied Surface Science*, **150**, 58–64.

Bonferoni M.C., Cerri G., de' Gennaro M., Juliano C. & Caramella C. (2007) Zn^{2+}-exchanged clinoptilolite-rich rock as active carrier for antibiotics in

https://doi.org/10.1180/clm.2019.23 Published online by Cambridge University Press

anti-acne topical therapy: *in-vitro* characterization and preliminary formulation studies. *Applied Clay Science*, **36**, 95–102.

Cagomoc C. & Vasquez Jr M. (2016) Enhanced chromium adsorption capacity *via* plasma modification of natural zeolites. *Japanese Journal of Applied Physics*, **56**, 01AF02.

Carretero M.I. & Pozo M. (2009) Clay and non-clay minerals in the pharmaceutical industry: part 1. Excipients and medical applications. *Applied Clay Science*, **46**, 73–80.

Cerri G., de' Gennaro M., Bonferoni M.C. & Caramella C. (2004) Zeolites in biomedical application: Zn-exchanged clinoptilolite-rich rock as active carrier for antibiotics in anti-acne topical therapy. *Applied Clay Science*, **27**, 141–150.

Cerri G., Farina M., Brundu A., Dakovic A., Giunchedi P., Gavini E. & Rassu G. (2016) Natural zeolites for pharmaceutical formulations: preparation and evaluation of a clinoptilolite-based material. *Microporous and Mesoporous Materials*, **223**, 58–67.

Ciobanu G., Carja G. & Ciobanu O. (2007) Preparation and characterization of polymer zeolite nanocomposite membranes. *Materials Science and Engineering C*, **27**, 1138–1140.

Concepcion-Rosabal B., Rodriguez-Fuentes N., Bogdanchikova N., Bosch P., Avalos M. & Lara V.H. (2005) Comparative study of natural and synthetic clinoptilolites containing silver in different states. *Microporous Mesoporous Materials*, **86**, 249–255.

Dardir F., Mohamed A., Abukhadra M.R., Ahmed E.A. &. Soliman M.F. (2018) Cosmetic and pharmaceutical qualifications of Egyptian bentonite and its suitability as drug carrier for Praziquantel drug. *European Journal of Pharmaceutical Sciences*, **115**, 320–329.

Demirci S., Ustaoglu Z., Yilmazer G. & Sahin F. (2013) Antimicrobial properties of zeolite-X and zeolite-A ion-exchanged with silver, copper, and zinc against a broad range of microorganism. *Applied Biochemistry and Biotechnology*, **172**, 1652–1662.

Dizaj S., Lotfipour F., Barzegar-Jalali M., Zarrintan M.H. & Adibkia K. (2014) Antimicrobial activity of the metals and metal oxide nanoparticles. *Materials Science and Engineering C*, **44**, 278–284.

European Pharmacopoeia (2005) *Bentonite, 5th edn*. European Pharmacopoeia, Strasbourg, France.

Ferreira L., Fonseca A., Botelho G., Almeida-Aguiar C. & Neves I.S. (2012) Antimicrobial activity of faujasite zeolites doped with silver. *Microporous and Mesoporous Materials*, **160**, 126–132.

Ghadiri M., Chrzanowski W. & Rohanizadeh R. (2015) Biomedical applications of cationic clay minerals. *RSC Advance*, **5**, 29467.

Grundy H. & Ito J. (1974) The refinement of the crystal structure of a synthetic non-stoichiometric Sr-feldspar. *American Mineralogist*, **59**, 1319–1326.

Inoue Y., Hoshino M., Takahashi H., Noguchi T., Murata T., Kanzaki Y., Hamashima H. & Sasatsu M. (2002) Bactericidal activity of Ag-zeolite mediated by reactive oxygen species under aerated conditions. *Journal of Inorganic Biochemistry*, **92**, 37–42.

Iqbal N., Abdul Kadir M., Iqbal S., Abd Razak S.I., Rafique M.S., Bakhsheshi-Rad H.R., Hasbullah Idris M., Khattak M.A., Raghavendran H.R.B. & Abbas A.A. (2016) Nano-hydroxyapatite reinforced zeolite ZSM composites: a comprehensive study on the structural and *in vitro* biological properties. *Ceramics International*, **42**, 7175–7182.

Levien L., Prewitt C. & Weidner D. (1980) Structure and elastic properties of quartz at pressure P = 61.4 kbar. *American Mineralogist*, **65**, 920–930 .

Li Y., Jiao Y., Li X. & Guo Z. (2015) Improving the osteointegration of Ti_6Al_4V by zeolite MFI coating. *Biochemical and Biophysical Research Communications*, **460**, 151–156.

Mansouri N., Rikhtegar N., Panahi H.A., Atabi F. & Shahraki B.K. (2013) Porosity, characterization and structural properties of natural zeolite–clinoptilolite as a sorbent. *Environment Protection Engineering*, **39**, 139–152.

Martucci A., Sacerdoti M., Cruciani G. & Dalconi C. (2003) *In situ* time resolved synchrotron powder diffraction study of mordenite. *European Journal of Mineralogy*, **15**, 485–493.

Moisan M., Barbeau J., Crevier M., Pelletier J., Philip N. & Saoudi B. (2002) Plasma sterilization. Methods and mechanisms. *Pure and Applied Chemistry*, **74**, 249–255.

Montallana A., Cruz C. & Vasquez Jr M (2018) Antibacterial activity of copper-loaded plasma-treated natural zeolites. *Plasma Medicine*, **8**, 1–10.

Namekawa K., Shreiber M., Aoyagi T. & Ebara M. (2014) Fabrication of zeolite polymer composite nanofibers for removal of uremic toxins from kidney failure patients. *Biomaterials Science*, **2**, 674–679.

Navratil Z., Trunec D., Smid R. & Lazar L. (2006) A software for optical emission spectroscopy-problem formulation and application to plasma diagnostics. *Czechoslovak Journal of Physics*, **56**, B944–B951.

Ninan N., Grohens Y., Elain A., Kalarikkal N. & Thomas S. (2013) Synthesis and characterization of gelatin/zeolite porous scaffold. *European Polymer Journal*, **49**, 2433–2445.

Nolan H., Sun D., Falzon B.G., Chakrabarti S., Padmanaba D.B., Maguire P., Mariotti D., Yu T., Jones D., Andrews G. & Sun D. (2018) Metal nanoparticle–hydrogel nanocomposites for biomedical applications – an atmospheric pressure plasma synthesis approach. *Plasma Processes and Polymers*, **15**, e1800112.

Olegario-Sanchez E. (2016) *Characterization and modification of Philippine natural zeolites by copper loading for environmental remediation by adsorption of hydrogen sulfide gas*. Master's thesis. University of the Philippines-Diliman, Quezon City, Philippines.

Olegario-Sanchez E. & Pelicano C. (2017) Characterization of Philippine natural zeolite and its application for heavy metal removal from acid mine drainage (AMD). *Key Engineering Materials*, **737**, 407–411.

Olegario E., Pelicano C., Dahonog L. & Nakajima H. (2019) Novel ZnO nanostructures on Philippine natural zeolite (PNZ) framework designed *via* thermal decomposition process of solution-based $ZnCl_2$ precursor. *Materials Research Express*, **6**, 015005.

Osonio A. & Vasquez Jr M. (2018) Plasma-assisted reduction of silver ions impregnated into a natural zeolite framework. *Applied Surface Science*, **432**, 156–162.

Ramasubramanian K., Severance M., Dutta P. & Ho W. (2015) Fabrication of zeolite/polymer multilayer composite membranes for carbon dioxide capture: deposition of zeolite particles on polymer supports. *Journal of Colloid Interface Science*, **452**, 203–214.

Taaca K. & Vasquez Jr M (2017) Fabrication of Ag-exchanged zeolite/chitosan composites and effects of plasma treatment. *Microporous and Mesoporous Materials*, **241**, 383–391.

Taaca K. & Vasquez Jr M (2018) Hemocompatibility and cytotoxicity of pristine and plasma-treated silver-zeolite–chitosan composites. *Applied Surface Science*, **432**, 324–331.

Taaca K., Olegario-Sanchez M. & Vasquez Jr M (2017) Antibacterial properties of Ag-exchanged Philippine natural zeolite–chitosan composites. *AIP Conference Proceedings*, **1901**, 030015.

Tomasevic-Canovic M. (2005) Purification of natural zeolite–clinoptilolite for medical application – extraction of lead. *Journal of Serbian Chemical Society*, **70**, 1335–1345.

US Pharmacopeia (2007) *US Pharmacopeial Convention*, Rockville, MD. (a) Bentonite, 1066; (b) purified bentonite, 1067; (c) microbial limit test. 83.

Uygun A., Kiristi M., Oksuz L., Manolache S. & Ulusoy S. (2011) RF hydrazine plasma modification of chitosan for antibacterial applications. *Carbohydrate Research*, **346**, 259–265.

Xiu Z.-m., Zhang Q.-b., Puppala H.L., Colvin V.L. & Alvarez P.J.J. (2012) Negligible particle-specific antibacterial activity of silver nanoparticles. *Nano Letters*, **12**, 4271–4275.

Yu L., Gong J., Zeng C. & Zhang L. (2013) Preparation of zeolite-A/chitosan hybrid composites and their bioactivities and antimicrobial activities. *Materials Science and Engineering C*, **33**, 3652–3660.

Zhang Y., Yan W., Sun Z., Pan C., Mi X., Zhao G. & Gao J. (2015) Fabrication of porous zeolite/chitosan monoliths and their applications for drug release and metal ions adsorption. *Carbohydrate Polymers*, **117**, 657–665.

https://doi.org/10.1180/clm.2019.23 Published online by Cambridge University Press